

# Spectroscopic observations of the interacting massive binary AQ Cassiopea

C. Ibanoglu<sup>a</sup>, Ö. Çakırlı<sup>a,\*</sup>, E. Sipahi<sup>a</sup>

<sup>a</sup>*Ege University, Science Faculty, Astronomy and Space Sciences Dept., 35100 Bornova, İzmir, Turkey.*

---

## Abstract

New spectroscopic observations of the double-lined eclipsing binary AQ Cas are presented. All available spectroscopic and photometric observations have been analysed for the fundamental properties of the components. Analyses show that the system consists of a massive primary with a mass of  $17.63 \pm 0.91 M_{\odot}$  and radius of  $13.48 \pm 0.64 R_{\odot}$  and a secondary with  $12.56 \pm 0.81 M_{\odot}$  and radius of  $23.55 \pm 0.73 R_{\odot}$ , corresponding spectral types of B0.5( $\pm 2$ ) II-III + B3( $\pm 1$ ) II. The secondary star fills its corresponding Roche lobe and mass transfer to the primary star is going on. This stream considerably does affect the photometric observations both starting from the second quarter up to the first contact of primary eclipse and just at the second maximum. Thus, the light curve is distorted and tightly depended on the wavelength of the observations. The available multi passband light curves have been analysed by taking the stream effects, as either hot or cool spots, into account. The comparison of the models and observations in the  $\log (L/L_{\odot}) - \log T_{eff}$

---

\*Corresponding author

*Email address:* omur.cakirli@gmail.com, Tel:+90 (232) 3111740, Fax:+90 (232) 3731403 (Ö. Çakırlı)

and  $\log g - \log T_{eff}$  diagrams clearly shows that the more massive star is consistent with models and is predicted to be close to the phase of hydrogen shell ignition. Average distance to the system is estimated as  $4150 \pm 240$  pc using the BVJHK magnitudes and V-passband extinction.

*Keywords:* Binaries Eclipsing – stars: fundamental parameters Individual method:spectroscopy

---

## 1. Introduction

**A massive star with a mass higher than 8-9  $M_{\odot}$  evolves through all cycles of nuclear burning up to iron when a core collapse supernova is formed. Such high mass stars undergo a strong loss of mass by the stellar wind which decreases their mass during nuclear evolution.** Observations of many massive stars have shown that the mass loss is larger for the more massive stars. The mass losses are so large that the outer atmospheres are removed and the convective cores may become visible at the surface. In this way some elements processed by nuclear reactions are carried out to the surface of a star. Spectroscopic observations of massive stars at advanced evolutionary stages reveal that the outer layers are enhanced in helium, carbon, nitrogen and oxygen. The evolutionary tracks are considerably different for the mass losing stars than those at constant mass (De Loore & Doom, 1992). When a star has a close companion its structure and evolution are significantly changed. While mass and chemical composition of a star define its evolution in the case of a binary system the total mass, the mass-ratio and the orbital period would affect its evolution. The mutual interaction between the components may cause to mass and angu-

lar momentum exchange which result in changes in the mass-ratio and the orbital period of the system. Although a number of the differences between the single and binary stars are well understood several are still in discussion, especially for massive binary stars.

Podsiadlowski, Joss & Hsu (1992) have investigated in detail how binary interaction affects the pre-supernova evolution of massive close binaries and the resulting supernova explosions. About 30 percent of all massive **stars are substantially** affected by interactions with close binary companions. Further evolution of a close binary system is tightly depended upon the mass and angular momentum loss. Eggleton (2000) called attention, for the first time, that mass and subsequent angular momentum loss significantly affect binary evolution. Sarna (1993) have shown that during evolution of  $\beta$  Per 15% of the initial total mass about two of third of the mass lost and 30 % of the total angular momentum were lost. Van Rensbergen his collaborators van Rensbergen (2003) have shown that *conservative* calculations cannot produce Algols with large mass-ratios.

Recently Torres, Andersen, & Giménez (2010) collected accurate masses and radii for the components of 95 double-lined detached binary systems. Their criterion was such that the mass and radius of both stars should be determined within an accuracy of 3 percent or better. The number of stars is decreasing in both directions towards the massive stars ( $M > 10 M_{\odot}$ ) and low-mass stars ( $M < 1 M_{\odot}$ ). In the last three years the number of low-mass stars for which mass and radius determined are considerably increased (see for example (Çakırlı, Ibanoglu, & Sipahi, 2013a,b)). Still there are some debates about the formation mechanism and evolution of massive binaries. Therefore,

we initiated a spectroscopic study for the massive binary systems.

AQ Cas is a semi-detached,  $\beta$  Lyrae type eclipsing binary with an orbital period of 11.721 days. Its spectra were obtained by Struve (1946) and the components were classified as B3 and B9. First photometric observations made by Olson (1985) and Nha & Chun (1988). Later on *UBV* observations and *I(Kron)uvby* light curves were published by Lee et al. (1993) and Olson (1994), respectively. There is large light variations between eclipses and light curve has a deep totality lasting about ten hours. In addition, light curves are significantly asymmetric which appears to tightly depended on the wavelength. About 40 years later some spectra of the system were obtained by Lee et al. (1993). These spectra showed the traces of both stream and rotation effects.

We report here spectroscopic observations which are added to the previous data and analysed together with the photometric observations for obtaining accurate masses and radii of the components. In addition, we have interpreted all available photometric and spectroscopic data on AQ Cas for understanding its present structure and evolution as well as physical properties of the stars. We also discuss the plausible causes of asymmetries in the observed multi passband light curves of the system.

## 2. Spectroscopic observations

Optical spectroscopic observations of the AQ Cas were obtained with the Turkish Faint Object Spectrograph Camera (TFOSC)<sup>2</sup> attached to the 1.5

---

<sup>2</sup><http://tug.tug.tubitak.gov.tr/rtt150.tfosc.php>

m telescope in July, 2010 under good seeing conditions. Further details on the telescope and the spectrograph can be found at <http://www.tug.tubitak.gov.tr>. The wavelength coverage of each spectrum was 4000-9000 Å in 12 orders, with a resolving power of  $\lambda/\Delta\lambda \sim 7000$  at 6563 Å and an average signal-to-noise ratio (S/N) was  $\sim 120$ . We also obtained high S/N spectra of several early type standard stars 21 Cyg,  $\tau$  Her, HR 153 and 21 Peg for use as templates in derivation of the radial and rotational velocities. The electronic bias was removed from each image and we used the **'crreject' (IRAF-immatch-imcombine-"Type of rejection")** combineoption for cosmic ray removal. Thus, the resulting spectra were largely cleaned from the cosmic rays. The echelle spectra were extracted and wavelength calibrated by using Fe-Ar lamp source with help of the IRAF ECHELLE (Tonry & Davis, 1979) package.

### 2.1. Radial velocities

To derive the radial velocities, the eleven spectra obtained for the system are cross-correlated against the template spectra of standard stars on an order-by-order basis using the FXCOR package in IRAF (Simkin, 1974).

The spectra showed two distinct cross-correlation peaks in the quadratures, one for each component of the binary. Thus, both peaks are fitted independently with a *Gaussian* profile to measure the velocities and their errors for the individual components. If the two peaks appear blended, a double Gaussian was applied to the combined profile using *de-blend* function in the task. For each of the eleven observations we then determined a weighted-average radial velocity for each star from all orders without significant contamination by telluric absorption features. Here we used as weights the inverse of the variance of the radial velocity measurements in each order,

as reported by FXCOR.

Since the orbital period of the system is considerably longer and the totality lasts about ten hours it is hard to obtain reliable times of mid-eclipse. Therefore, only nine photoelectric times for primary eclipse are collected from the GATEWAY data-base. A linear least-squares fit to the data yields the following ephemeris

$$\text{Min I} = \text{HJD } 2453920.897(27) + 11^d.72107(18) \times E$$

where the bracketed quantity is the uncertainty in the last digits of the preceding number.

The heliocentric radial velocities for the primary ( $V_p$ ) and the secondary ( $V_s$ ) components are listed in Table 1, along with the dates of observations and the corresponding orbital phases computed with the new ephemeris given above. The velocities in this table have been corrected to the heliocentric reference system by adopting a radial velocity value for the template stars. The radial velocities are plotted against the orbital phase in Fig. 1, together with the radial velocities obtained by Lee et al. (1993) (empty circles). The three velocities of the primary star in phases 0.12-0.16 and nine velocities in phases 0.81-0.90 are affected from gas stream and rotation. In addition, the velocities of both components in the orbital phase about 0.38 are systematically deviated from the orbit. Therefore, thirteen measurements for the primary and one for the secondary are not plotted in Fig. 1. There is no systematic difference between our and their remaining measurements.

We analysed all the radial velocities for the initial orbital parameters using the RVSIM software program (Kane, Schneider, & Ge, 2007). Figure 1 shows the best-fit orbital solution to the radial velocity data. The re-

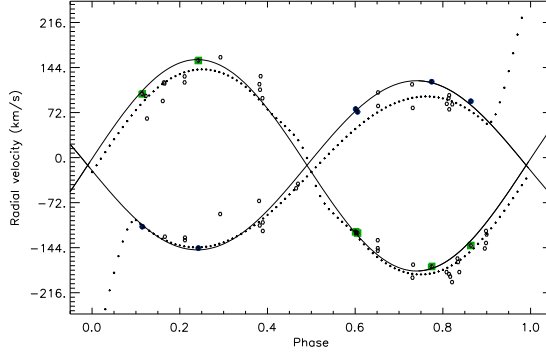


Figure 1: Radial velocities for the components of AQ Cas. Symbols with error bars show the radial velocity measurements for the components of the system (primary: filled circles, secondary: open squares). The velocities measured by Lee et al. (1993) are shown by empty circles.

sults of the analysis are as follow:  $\gamma = -16.6 \pm 2.2 \text{ km s}^{-1}$ ,  $K_1 = 120.9 \pm 3.9$  and  $K_2 = 169.6 \pm 3.4 \text{ km s}^{-1}$  with circular orbit. Using these values we estimate the projected orbital semi-major axis and mass ratio as:  $a \sin i = 67.4 \pm 1.2 R_\odot$  and  $q = \frac{M_2}{M_1} = 0.713 \pm 0.027$ .

## 2.2. Rotational velocity

The width of the cross-correlation profile is a good tool for the measurement of  $v \sin i$  (see, e.g., Queloz et al. (1998)). The rotational velocities ( $v \sin i$ ) of the two components were obtained by measuring the FWHM of the CCF peaks in nine high-S/N spectra of AQ Cas acquired close to the quadratures, where the spectral lines have the largest Doppler-shifts. In order to construct a calibration curve FWHM– $v \sin i$ , we have used average spectra of the  $\iota$  Psc and  $\tau$  Her. The FWHM of the CCF peak was measured and the FWHM– $v \sin i$  calibration was established. The  $v \sin i$  values of the

Table 1: Heliocentric radial velocities of AQ Cas. The columns give the heliocentric Julian date, the orbital phase (according to the ephemeris in §2), the radial velocities of the two components with the corresponding standard deviations.

HJD 2400000+	Phase	Star 1		Star 2	
		$V_p$	$\sigma$	$V_s$	$\sigma$
56131.4953	0.6010	77.5	3.2	-118.6	4.3
56131.5470	0.6054	73.2	3.4	-120.6	4.6
56133.5279	0.7744	121.4	2.8	-174.0	3.8
56134.5740	0.8637	90.1	3.1	-140.5	4.2
56137.5130	0.1144	-110.4	3.1	101.9	4.4
56326.5500	0.2423	-144.7	2.1	155.3	3.0

components of AQ Cas were derived from the FWHM of their CCF peaks. We find  $287 \pm 5 \text{ km s}^{-1}$  for the primary and  $98 \pm 9 \text{ km s}^{-1}$  for the secondary star.

### 3. Light curves and their analyses

The first *uvbyI* photoelectric observations of AQ Cas were obtained by Olson (1985). The resulting light curves are significantly variable in the sense that the light just before the first contact is depressed by about 0.1 mag in the u-passband relative to the fourth contact. This difference is decreased towards longer wavelengths. The light loss before the first contact is attributed to the stream seen projected against the gainer. In addition, some light fluctuations are seen beginning from mid-secondary-eclipse. Additional observations of AQ Cas were obtained by Olson & Bell (1989) using the same filter set. First wide passband UBV observations obtained between 1982 and



1989 were published by Lee et al. (1993). Despite the large fluctuations in fluxes the average shape of the light curve is revealed. Their BV light curves are almost symmetric except the secondary eclipse. The ingress is steeper than the egress. Five-color intermediate-band *uvbyI* observations of the system were obtained by Olson (1994). Thus, almost complete multi-passband light curves were revealed. The asymmetry in the light curves was increasing towards the shorter wavelengths. In addition, the asymmetry is in an opposite direction as we go to the longer wavelengths. In the u-passband light curve was the most asymmetrical shape, being the first maximum dimmer than the second. However, the I-passband light curve is almost symmetric, the light level at the first maximum is slightly higher than that of the second maximum.

The observations of AQ Cas were also made by two familiar surveys. The R-passband light curve was obtained by the Northern Sky Variability Survey (NSVS) (Wozniak et al., 2004). The light curve is very similar to that obtained by Olson in the *I*-passband. The last V-passband light curve of AQ Cas was obtained by the International Gamma-Ray Astrophysics Laboratory (*INTEGRAL*) mission (Alfonso-Garzón et al., 2012). With 3139 V-passband measurements the shape of the light variation is clearly defined. The magnitude of the system appears to reach maximum just at phase 0.75 and a steady decline up to the first contact is seen. The egress of the primary eclipse is steeper than that of egress. In contrary the egress of the secondary eclipse is steeper than that of egress. Both the minima and maxima are asymmetric. In Fig.2 we show Olson-I Lee-V, NSVS-R and *INTEGRAL*-V light curves of AQ Cas.

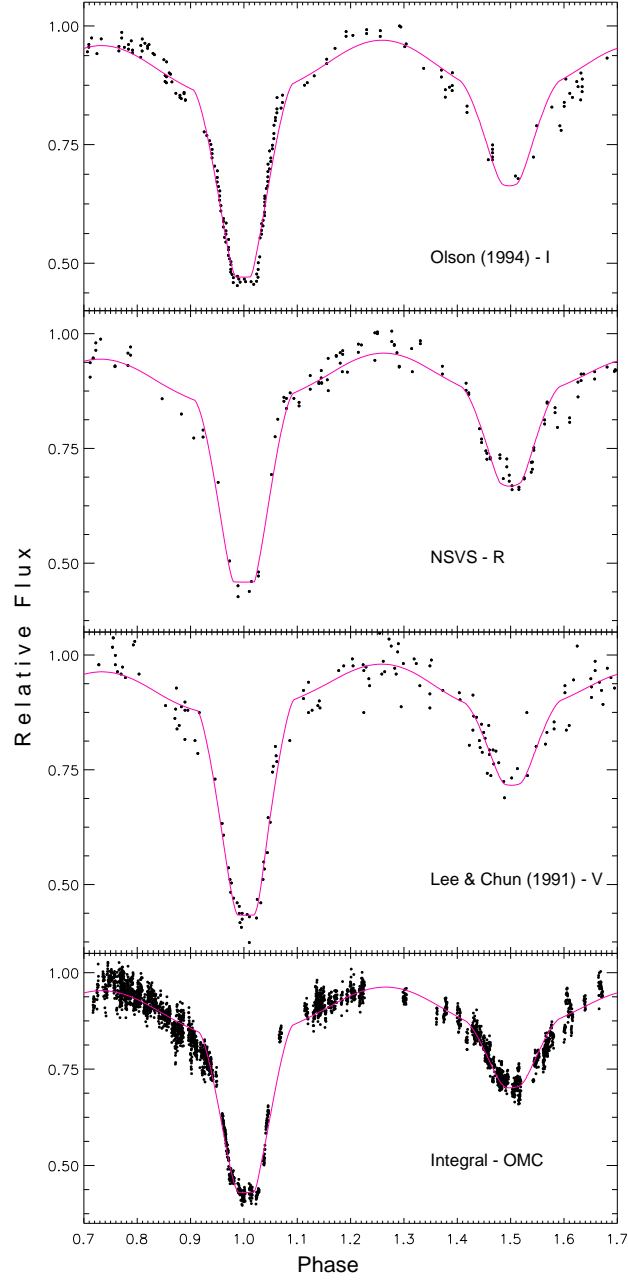


Figure 2: The Olson's  $I$ , Lee's  $V$ , NSVS- $R$  and *INTEGRAL*- $V$  light curves of AQ Cas. The continuous lines show the best-fit model.

Since the analysis of the light curves is depended on the effective temperature of the hotter component try to constrain the effective temperature and spectral type of the primary star using the *uvbyI* and *JHK* magnitudes. The intermediate passband colors of both components are already given by Olson (1985) with an interstellar reddening of  $E(b-y)=0.64$  mag.  $V=10.31$ ,  $B-V=0.53$ ,  $J-H=0.182\pm0.039$  and  $H-K=0.170\pm0.031$  mag were taken from SIMBAD data-base and 2MASS catalog. Using the colors and reddening we estimate a spectral type and effective temperature of the primary star as B0.5III and  $T_{\text{eff}} = 27\,000\pm1000\text{K}$  by color-spectral type-effective temperature relations given by de Jager & Nieuwenhuijzen (1987), Drilling & Landolt (2000) and Tokunaga (2000).

We used the eclipsing binary light curve modeling algorithm of Wilson & Devinney (1971), as implemented in the PHOEBE code of Prša & Zwitter (2005). The non-linear square-root limb-darkening and bolometric limb-darkening are adopted from Diaz-Cordoves, Claret,& Gimenez (1995) van Hamme (1993), respectively. The gravity-brightening coefficients  $g_1=g_2=1.0$  and albedos  $A_1=A_2=1.0$  were assumed for the components. The rotational velocity of the primary star is measured about  $287\text{ km s}^{-1}$ , being five times faster than synchronous rotation. While the less massive star is appeared to be synchronous with the orbital one, for the more massive component  $F_1=5$  is assumed. Using a trial-error method, we obtained a set of parameters which represented the observed light curves. This preliminary analysis shows that the secondary component fills its corresponding Roche lobe. Therefore, Mode-5 was adopted.

The shapes of the light curves are tightly depended on the wavelength.

Photometric and spectroscopic observations clearly show that there is a mass stream from the secondary to the primary star. The stream impacts directly to the more massive star. This impact region is seen by the observer just at the second quarter. Therefore, additional light is observed. Thereafter, the stream begins to absorb the light of the primary star which causes light loss. On the other hand, during the second quarter the observer receives light from the stream in addition to both stars. Therefore, the brightness of the system is slightly increased. All these effects can only be modelled by the hot or cool spots in the Wilson-Devinney code.

The adjustable parameters in the light curves fitting were the orbital inclination, the surface potential of the primary star, the effective temperature of the secondary, and the wavelength-dependent luminosity of the hotter star, the zero-epoch offset. Our final results are listed in Table 2. The uncertainties assigned to the adjusted parameters are the internal errors provided directly by the code. The computed light curve corresponding to the simultaneous light-velocity solution is compared with the observations in Fig. 2.

Combining the results of radial velocities and light curves analyses we have calculated the absolute parameters of the stars. The fundamental stellar parameters for the components such as masses, radii, luminosities are listed in Table 3 together with their formal standard deviations. The standard deviations of the parameters have been determined by JK TABSDIM<sup>3</sup> code, which calculates distance and other physical parameters using several different sources of bolometric corrections (Southworth et al., 2005). The

---

<sup>3</sup>This can be obtained from <http://http://www.astro.keele.ac.uk/~jkt/codes.html>

Table 2: Results of the simultaneous analyses of the Olson’s  $I$ , Lee’s  $V$ , NSVS- $R$  and *INTEGRAL-V* light curves for AQ Cas light curves.

Parameters	Adopted
$i^\circ$	$84.41 \pm 0.40$
$T_{eff_1}$ (K)	17 000[Fix]
$T_{eff_2}$ (K)	$16\,700 \pm 400$
$\Omega_1$	$5.781 \pm 0.166$
$\Omega_2$	$4.640 \pm 0.155$
$r_1$	$0.1995 \pm 0.0088$
$r_2$	$0.3484 \pm 0.0090$
$\frac{L_1}{(L_1+L_2)}$ (Olson- $I$ )	$0.4028 \pm 0.0101$
$\frac{L_1}{(L_1+L_2)}$ (Lee- $V$ )	$0.4584 \pm 0.0114$
$\frac{L_1}{(L_1+L_2)}$ (NSVS- $R$ )	$0.4190 \pm 0.0119$
$\frac{L_1}{(L_1+L_2)}$ ( <i>INTEGRAL-V</i> )	$0.4424 \pm 0.0023$
$\sigma$	0.032

mass for the primary of  $M_P = 17.63 \pm 0.91 M_\odot$  and secondary of  $M_S = 12.56 \pm 0.81 M_\odot$  are consisting of a B0.5II-III star and an evolved B3 super-giant star (Drilling & Landolt , 2000).

The interstellar reddening is estimated by Olson (1985) as  $E(b-y)=0.64$  mag which corresponds to  $E(B-V)=0.88$  mag. Using this value and the BVR-JHK magnitudes and bolometric corrections given by Girardi et al. (2002) we estimated an average distance to the system as  $4150 \pm 240$  pc.

#### 4. Results and Conclusions

First spectroscopic observations were made by Struve (1946) who estimated minimum mass for the components as  $11 M_\odot + 15 M_\odot$  and spectral type of B3+B9. Almost a half century later Lee et al. (1993) derived absolute physical properties of the component stars using their spectroscopic and photometric observations. The masses and radii are found as  $18.1 M_\odot + 12.9 M_\odot$

Table 3: Properties of the AQ Cas components

Parameter	Primary	Secondary
Mass ( $M_{\odot}$ )	$17.63 \pm 0.91$	$12.56 \pm 0.81$
Radius ( $R_{\odot}$ )	$13.48 \pm 0.64$	$23.55 \pm 0.73$
$T_{eff}$ (K)	$27\,000 \pm 1000$	$16\,700 \pm 400$
$\log (L/L_{\odot})$	$4.940 \pm 0.076$	$4.590 \pm 0.050$
$\log g$ (cgs)	$3.425 \pm 0.039$	$2.793 \pm 0.026$
Spectral Type	B0.5( $\pm 2$ )II-III	B3( $\pm 1$ )II
$(v \sin i)_{obs.}$ (km s $^{-1}$ )	$287 \pm 5$	$98 \pm 9$
$(v \sin i)_{calc.}$ (km s $^{-1}$ )	$15 \pm 1$	$4 \pm 1$
$a$ ( $R_{\odot}$ )	$67.59 \pm 1.21$	
$V_{\gamma}$ (km s $^{-1}$ )	$-9 \pm 1$	
$q$	$0.713 \pm 0.027$	
$d$ (pc)	$4150 \pm 240$	

and  $13.5R_{\odot} + 25.8R_{\odot}$ , respectively. They classify the system as a semi-detached eclipsing binary without any conclusion about the spectral types of the components. A year later Olson (1994) published the five- color light curves and their analysis. He also measured radial velocities of the cooler star from the spectroscopic observations of OI  $\lambda 7774$  line. He estimates masses for the components  $16.6M_{\odot}$  and  $4.72M_{\odot}$ , radii of  $7.55R_{\odot}$  and  $16.6R_{\odot}$ . Polushina (2004) published a catalog of massive close binaries with early-type components which includes AQ Cas. The spectral types and masses of the components are given as O8.5III+O8.5III and  $29.5M_{\odot} + 24.6M_{\odot}$ . Our re-analyses of all available photometric and spectroscopic data yield the mass, absolute radius and effective temperature for the primary and secondary stars are  $17.63 \pm 0.91M_{\odot}$ ,  $13.48 \pm 0.64R_{\odot}$ ,  $27\,000 \pm 1000$ , and  $12.56 \pm 0.81M_{\odot}$ ,  $23.55 \pm 0.73$ ,  $16\,700 \pm 400$ , respectively. These values correspond to the spectral type of B0.5III and B3II. Thus, the masses of the components have been derived with an accuracy of 5 percent for the primary and 6 percent for the secondary and radii

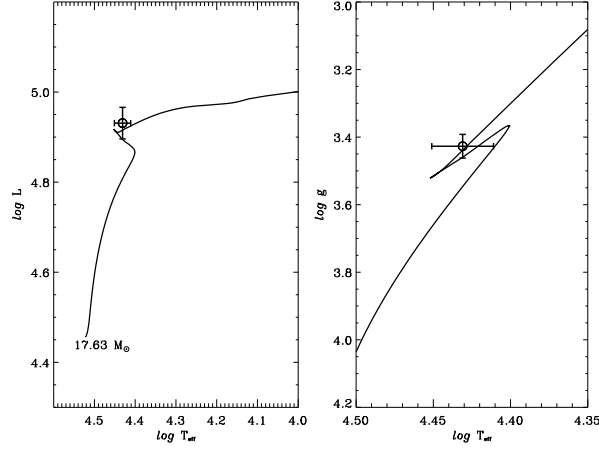


Figure 3:  $\log (L/L_{\odot})$ - $\log T_{eff}$  (left panel) and  $\log g - \log T_{eff}$  (right panel) plots of the primary component of AQ Cas compared with Ekström et al. (2012) models for  $Z=0.014$ .

of 5 percent and 3 percent, respectively.

In Fig.3 we plot the location of the primary star of AQ Cas in  $\log (L/L_{\odot})$ - $\log T_{eff}$  (left panel) and  $\log g - \log T_{eff}$  (right panel) diagrams with error bars. The evolutionary tracks of a  $17.63 M_{\odot}$  have been constructed by Ekström et al. (2012) models for  $X=0.720$ ,  $Y=0.266$  and  $Z=0.014$ . Stellar rotation is taken into account in their models. Despite their models provide a good description of the average evolution of non-interacting single stars, locations of the gainer are in good agreement with evolutionary tracks as seen in both panels. The primary star is predicted to be close to the phase of hydrogen shell ignition.

AQ Cas is a classical Algol. While the more massive star is filling its Roche lobe by about 0.52 the less massive star completely fills and overflows its lobe. A mass transfer is taking place from the less massive (donor) star to the more massive (gainer). Mass flows from the inner Lagrangian point and the trajec-

tory and properties of the mass-transferring stream are studied in detail by Lubow & Shu (1975). The type of accretion structures can be predicted from position of a gainer in the well-known *radius – massratio* diagram. If the orbital period of a system is too long, the fractional radius will be too small that mass transfer results in classical accretion disks. If the fractional radius of the gainer is sufficiently large, stream directly strikes its photosphere. This impact leads to the formation of a hot impact region and variable accretion structures. The gainer of the AQ Cas, with  $r=0.2$  and  $q=0.7$ , locates in the region of impactors (see Fig.3 in Dervişoğlu, Tout,& Ibanoglu (2010)). Although its position is close to U Cep in the  $r – q$  plane, the mass-ratio and orbital period for AQ Cas are very different. It seems that AQ Cas is a mass-transferring system with higher mass-ratio and longer orbital period.

Recently Dervişoğlu, Tout,& Ibanoglu (2010) studied spin angular momentum evolution of the accreting components of Algol-type interacting binaries. They demonstrate that a small amount of mass transfer leads to accumulation of enough angular momentum which spins the gainer up to its critical rotation velocity. Since the gainer is in Algols have radiative envelopes, angular momentum and mass loss are not taken place due to the enhanced magnetic activity, as are occurred in solar-type chromospherically active stars. Therefore, they take into account generation of magnetic fields in the radiative atmospheres in differentially rotating star and the possibility of angular momentum loss driven by strong stellar winds. Differential rotation induced by the accretion itself may produce stellar winds which carry away enough angular momentum to reduce their rotational velocities to the presently observed values. They suggest that this self consistent model



should be more effective in the angular momentum loss of long-period Algols. The rotational velocity of the gainer was measured as  $240 \text{ km s}^{-1}$  by Etzel & Olson (1993), and they estimate an  $F_1$  value of 7.3. We measured a rotational velocity of  $v_{rot} \sin i = 287 \pm 5 \text{ km s}^{-1}$  which is five times faster than synchronous rotation. As the mass of the gainer increases the rotation velocity is decreasing, as shown in their Fig.2. The  $F_1$  value found in this study is in agreement with their estimate for massive primaries with orbital periods longer than 5 days. As discussed by Ibanoglu et al. (2006) interacting Algols with  $q > 0.3$  and  $P > 5$  days have almost the same angular momentum to those of detached binaries. So, with a mass-ratio of 0.7 and an orbital period of 11.7 days the angular momentum loss during the evolution of AQ Cas is not too high. Comparison with the evolutionary tracks indicates similar results.

## Acknowledgments

We thank to TÜBİTAK National Observatory (TUG) for a partial support in using RTT150 telescope with project number 11BRTT150-198. We also thank to the staff of the Bakırlıtepe observing station for their warm hospitality. This study is supported by Turkish Scientific and Technology Council under project number 112T263 and 108T237. The following internet-based resources were used in research for this paper: the NASA Astrophysics Data System; the SIMBAD database operated at CDS, Strasbourg, France; TÜBİTAK ULAKBİM Süreli Yayınlar Kataloğu-TURKEY; and the arXiv scientific paper preprint service operated by Cornell University. The authors are indebted to the anonymous referee for his/her valuable suggestions which

improved the paper.

## References

- Alfonso-Garzón J., Domingo A., Mas-Hesse J. M., Giménez A., 2012, *A&A*, 548, A79
- Çakırlı Ö., Ibanoglu C., Sipahi E., 2013a, *MNRAS*, 429, 85
- Çakırlı Ö., Ibanoglu C., Sipahi E., 2013b, *NewA*, 20, 1
- de Jager C., Nieuwenhuijzen H., 1987, *A&A*, 177, 217
- De Loore C. W. H., Doom C., 1992, in *Structure and evolution of single and binary stars*, Dordrecht ; Boston : Kluwer Academic Publishers, p.242
- Dervişoğlu A., Tout C. A., Ibanoglu C., 2010, *MNRAS*, 406, 1071
- Diaz-Cordoves J., Claret A., Gimenez A., 1995, *A&AS*, 110, 329
- Drilling J. S., Landolt A. U., 2000, *Allen’s astrophysical quantities*, 4th ed. Edited by Arthur N. Cox. ISBN: 0-387-98746-0. Publisher: New York: AIP Press; Springer, 2000, p.381
- Eggleton P. P., 2000, *NewAR*, 44, 111
- Ekström S., et al., 2012, *A&A*, 537, A146
- Etzel P. B., Olson E. C., 1993, *AJ*, 106, 1200
- Fernandez J. M., Latham D. W., Torres G., Everett M. E., Mandushev G., Charbonneau D., O’Donovan F. T., Alonso R., Esquerdo G. A., Hergenther C. W, and Stefanik P. P., 2009, *ApJ*, 701, 764

- Girardi L., Bertelli G., Bressan A., Chiosi C., Groenewegen M. A. T., Marigo P., Salasnich B., Weiss, A., 2002, A&A, 391, 195
- Ibanoglu C., Soydogan F., Soydogan E., Dervişoğlu A., 2006, MNRAS, 373, 435
- Kane S. R., Schneider D. P., Ge J., 2007, MNRAS, 377, 1610
- Lee Y. S., Chun Y. W., Jeong J. H., Nha I. S., 1993, ASPC, 38, 298
- Lubow S. H., Shu F. H., 1975, ApJ, 198, 383
- Nha I.-S., Chun Y.-W., 1988, in Observations vs Physical Models for Close Binary Systems, Edited by K.C.Leung (Gordon and Breach, New York), 191
- Nidever D. L., Marcy G. W., Butler R. P., Fischer D. A., and Vogt S. S., 2002, ApJS, 141, 503
- Olson E. C., 1985, PASP, 97, 731
- Olson E. C., 1994, AJ, 108, 666
- Olson E. C., Bell D. J., 1989, PASP, 101, 907
- Podsiadlowski P., Joss P. C., Hsu J. J. L., 1992, ApJ, 391, 246
- Polushina T. S., 2004, A&AT, 23, 499
- Prša A., Zwitter T. 2005, ApJ, 628, 426P
- Queloz D., Allain, S., Mermilliod, J.-C., Bouvier, J., & Mayor, M., 1998, A&A, 335, 183

- Royer, F., Gerbaldi, M., Faraggiana, R., & Gomez, A. E. 2002, A&A, 381, 105
- Sarna M. J., 1993, MNRAS, 262, 534
- Simkin, S. J., 1974, A&A, 31, 129
- Southworth J., Smalley B., Maxted P. F. L., Claret A. & Etzel P. B. 2005, MNRAS, 363, 529
- Struve O., 1946, ApJ, 104, 253
- Tokunaga A. T., 2000, "Allen's astrophysical quantities", Fourth Edition, ed. A.N.Cox (Springer), p.143A
- Tonry J., & Davis M., 1979, AJ 84, 1511
- Torres G., Andersen J., Giménez A., 2010, A&ARv, 18, 67
- van Hamme, W. 1993 AJ, 106, 2096
- van Rensbergen W., 2003, ASSL, 298, 117
- Wilson R.E. & Devinney E.J., 1971, ApJ, 166, 605
- Wozniak P.R., Vestrand C.W., Akerlof R., et al., 2004, AJ, 127, 2436